

## Hybrid domain walls and antiferromagnetic domains in exchange-coupled ferromagnet/antiferromagnet bilayers

C. L. Chien,<sup>1</sup> V. S. Gornakov,<sup>2,3</sup> V. I. Nikitenko,<sup>1,2,3</sup> A. J. Shapiro,<sup>2</sup> and R. D. Shull<sup>2</sup>

<sup>1</sup>*Department of Physics and Astronomy, The Johns Hopkins University, Baltimore, Maryland 21218, USA*

<sup>2</sup>*National Institute of Standards and Technology, Gaithersburg, Maryland 20899, USA*

<sup>3</sup>*Institute of Solid State Physics, Russian Academy of Sciences, Chernogolovka 142432, Russia*

(Received 12 August 2002; revised manuscript received 21 March 2003; published 15 July 2003)

Magneto-optical imaging has revealed new features crucial for the understanding of the exchange bias phenomenon. We have observed hybrid domain walls consisting of ferromagnetic (FM) and antiferromagnetic sections and their evolution. The external magnetic field moves only the ferromagnetic section of the hybrid domain walls, leading to the formation of an exchange spring parallel to the interface. The nucleation and unwinding of the exchange spring occur at different locations and its propagation depends on the chirality of the FM domain walls. The stationary antiferromagnetic sections of the hybrid domain walls define the antiferromagnetic domains.

DOI: 10.1103/PhysRevB.68.014418

PACS number(s): 75.70.Cn, 75.30.Et, 75.50.Kj

The phenomenon of exchange bias between a ferromagnet (FM) and an antiferromagnet (AF) has been intensely studied in recent years,<sup>1-4</sup> prompted by the intriguing physics and its prominent role in spin-valve field sensing devices.<sup>5</sup> A unidirectional exchange anisotropy in the FM, as revealed by a shifted hysteresis loop, can be established in a FM/AF bilayer, most commonly by cooling the bilayer in a static external magnetic field from high to low temperatures, during which the AF order develops. Despite its importance, the understanding of the physics of exchange bias remains unsatisfactory. However, it has been recognized that the nature of the AF spin structure holds the key to the understanding of exchange bias.

Most theoretical models and experimental investigations of exchange bias have assumed a static AF spin structure for simplicity.<sup>1-4</sup> The exchange bias is the result of interactions between the FM layer and the uncompensated interfacial AF spin structure, while the remaining AF spin structure is assumed to be unchanged throughout the magnetization reversal process of the FM layer. Other theoretical and experimental studies of exchange bias have concluded that the AF spin structure could not be static.<sup>4,6-11</sup> In particular, Mauri *et al.* first showed that when the magnetization of the FM is reversed, the subsequent AF layers fan out into a spiraling AF spin structure as an exchange spring near the FM/AF interface.<sup>6</sup> Despite their crucial roles in exchange bias, the underlying AF spin structure and AF domains are not readily accessible to most experimental investigations. Furthermore, it has been demonstrated that the AF spin structure is drastically altered after the FM layer has been deposited.<sup>12</sup> Thus, the AF spin structure must be studied in FM/AF bilayers rather than AF layers in isolation.

The understanding of the exchange bias phenomenon and the central issue of the AF spin structure can be addressed through the reversal processes of the FM layer exchange coupled to the AF layer. In this work, we report on the observation of an acute asymmetry in the nucleation and orientation of the FM domain walls (DW) during reversal. We have also revealed the AF domains that are bounded by stationary AF domain walls and the existence of

hybrid FM/AF domain walls in the ground state. These observations demonstrate that the underlying AF spin structure forms an exchange spring, whose chirality dictates the asymmetry.

We have used a common FM/AF bilayer of Ni<sub>81</sub>Fe<sub>19</sub>(160 Å)/FeMn(300 Å) grown on a Cu seed layer of 300 Å deposited on a Si substrate. All layers are polycrystalline with grains several hundred angstrom in sizes. When the bilayer is cooled in the usual way under a static magnetic field from 400 to 300 K with a single-domain FM, the hysteresis loop measured by a vibrating sample magnetometer (VSM) at 300 K is shifted from  $H=0$ , as shown in Fig. 1(a). However, as discussed below, this most commonly achieved ground state is not suitable for revealing the underlying AF spin structure. Instead, when the same sample is first ac demagnetized in a field of decreasing magnitude to zero total magnetization at 400 K, and then cooled in zero magnetic field to 300 K, one observes two loops, shifted to either sides of  $H=0$ , as shown in Fig. 1(b).<sup>13</sup> This is because the ac demagnetization creates large stripe domains with opposite magnetizations, which acquire bias fields of opposite sign, as schematically shown in the inset of Fig. 1(b). This special ground state of stripe FM domains reveals the key features of exchange bias.

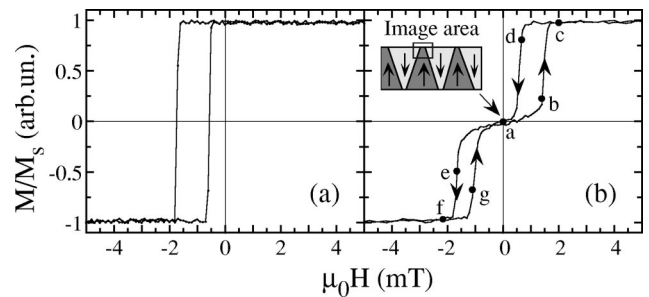


FIG. 1. Hysteresis loop of Ni<sub>81</sub>Fe<sub>19</sub>(160 Å)/FeMn(300 Å) at 300 K after (a) cooled in 1 T field from 400 to 300 K, and (b) ac demagnetized at 400 K and cooled in zero field to 300 K. Points  $a, b, c$ , etc. correspond to the domain patterns in Fig. 2. The domain pattern and the image area are shown in the inset.

The magneto-optical indicator film (MOIF) technique has been used to observe on a microscopic level the reversal processes. Imaging techniques that use an electron beam as in scanning electron microscopy, or a magnetic tip as in magnetic force microscopy, are strongly susceptible to external magnetic fields. These imaging techniques are usually administered in zero external field. In contrast, the MOIF technique allows the application of an external magnetic field during imaging throughout the reversal process. As described elsewhere, the MOIF method uses an iron garnet film with in-plane magnetization and a large Faraday effect placed directly above the sample.<sup>14</sup> Any stray magnetic field in the sample due to magnetization discontinuities at the sample edge, at FM domain walls, and at atomic defects causes magneto-optical Faraday effect in the indicator film. In the domain pattern below, the magnetization in each domain is directed from the “black” edge towards the “white” edge.

The MOIF microscope was focused on one area near the edge of the sample capturing three FM domains with two domain walls, as shown in Fig. 2(a). The image area is about  $1\text{ mm} \times 1.5\text{ mm}$ , and thus the size of the FM domain is macroscopically large. There are thousands of grains in each sub-mm-sized magnetic domain. When an external magnetic field is applied along the exchange anisotropy axis, the evolution of the domains are shown in Fig. 2 corresponding to the specific points on the double hysteresis loop, shown in Fig. 2(b) in the order of  $a \Rightarrow b \Rightarrow c \Rightarrow d \Rightarrow a \Rightarrow e \Rightarrow f \Rightarrow g \Rightarrow a$ .

We first describe the domain evolution for the positive loop. Starting from the demagnetized state of  $a$  shown in the middle of Fig. 2, upon applying a positive magnetic field  $H$  of increasing magnitude, the pattern evolves from  $a$  to  $c$  via  $b$ , where the central “down” domain reverses to “up.” This occurs with the invading domains (shown as white arrows) consuming the “up” regions. Returning from  $c$  to  $a$  via  $d$ , by applying a positive  $H$  of decreasing magnitude, the invading “down” domains reverse the central “up” domain. For the negative loop, the domain pattern changes from  $a$  to  $f$  via  $e$ . The invading “down” regions, marked by the white arrows, occur in the two outer domains until state  $f$  is reached. Upon returning from  $f$  to  $a$  via  $g$ , the two outer “down” domains reverse to “up.”

In an isolated FM layer without the AF layer, at symmetric points of the hysteresis loop, the domain patterns are the same but with reversed magnetization. This is because the same domain walls are pinned by the same *static* defects in both forward and backward reversal. In the FM layer exchange coupled to the AF layer, the domain patterns of  $d$  and  $e$  in Fig. 2 (likewise by comparing  $b$  and  $g$ ) are totally different. The domain patterns in Fig. 2 also reveal several new aspects of exchange bias. There is an asymmetry in the nucleation of the domains for forward and backward reversal. During reversal, only one of the two DW’s is shifted to accommodate the invading domains. This is clearly shown in  $b$ , in which the invading domains nucleate and propagate from the right DW, whereas in  $d$  the domains nucleate from the left DW. The same conclusion is reached by comparing  $e$  and  $g$ . Thus, there is an acute

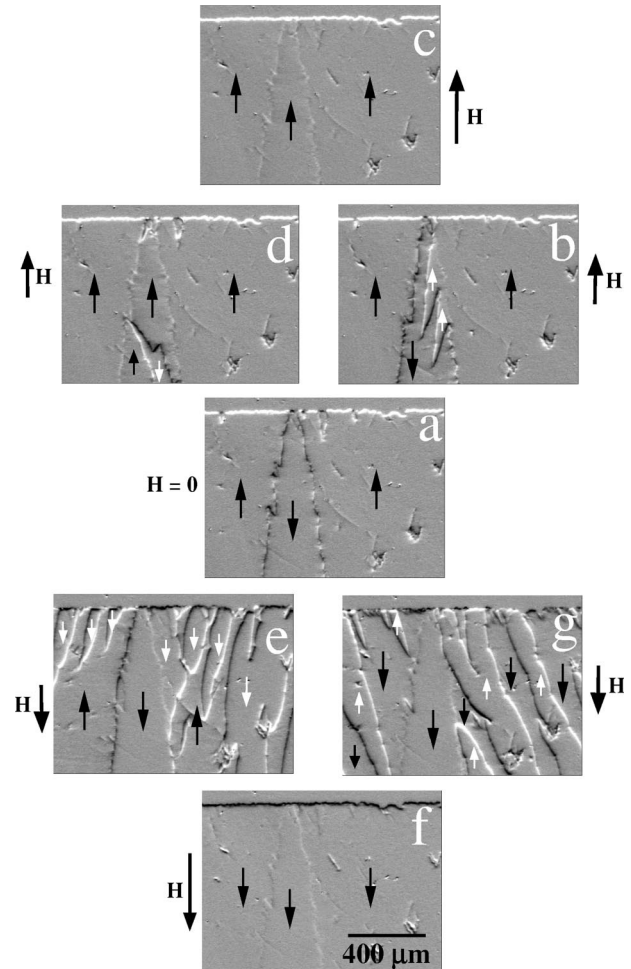


FIG. 2. MOIF image of domain patterns taken at various points ( $a, b, c$ , etc.) on the double hysteresis loop of Fig. 1(b) with the magnetic field  $\mu_0 H$  of (a) 0, (b) 1.8, (c) 6, (d) 0.6, (e)  $-1.2$ , (f)  $-6$ , (g)  $-0.35$  mT. The black arrows indicate the magnetization direction of the domains, whereas the white arrows indicate those of the invading domains.

asymmetry in both domain nucleation and domain wall propagation for forward and backward reversal. The acute asymmetry observed in the FM/AF bilayer vividly demonstrates that the underlying AF spin structure must not be static.

MOIF studies of the reversal processes of exchange-coupled FM/AF bilayers uncover yet another unusual phenomena. In Fig. 2, one observes by comparing  $b$  with  $d$  for the central domain that the invading domains are *not* along the easy axis. The invading domains in  $b$  slant to the left, while the invading domains in  $d$  slant to the right. The same conclusion is reached by comparing  $e$  and  $g$  for the invading domains in the two outer domains. Thus, there is a distinct chirality, an evidence of an exchange spring that winds and unwinds during forward and backward reversal.

In FM layers, isolated or exchange coupled, all the FM domain walls can be swept by an external magnetic field and the FM becomes a single domain. It is particularly revealing to compare Fig. 2(a), in which two FM DWs separate three

FM domains with opposite magnetizations, with the single-domain states of  $2c$  and  $2f$  of opposite magnetization. That  $c$  and  $f$  are single FM domains is unequivocal by noting the white edge in  $c$  and black edge in  $f$ . Most remarkably, even in the single-domain FM of  $c$  and  $f$ , there are still weaker but clearly visible contrasts at the original locations of the FM DW. In fact, an inspection of all the domain patterns in Fig. 2 shows that within the field range of about  $-2$  mT to  $+2$  mT, these contrasts at the same locations are always present regardless of the state of the FM domains or the magnetic field applied. These are the indications of the *stationary* AF DWs, which are not swept by the applied field, thus revealing the underlying AF domains. The weaker contrast of the AF DW is due to FM spin frustration near its intersection with the FM/AF interface. In this regard, the FM layer plays the role of a sensitive sensor through which stray fields at the AF DW can be detected.

The fact that the faint contrasts at the original locations of the FM DW persist, as shown in Figs. 2(c) and 2(f), after the FM layer has been aligned into a single domain state by a field of about 2 mT warrants further investigation. One might suspect that the faint contrasts might be due to certain irregularities in the FM layer, instead of the stationary AF DW to which we have attributed. Further imaging has been performed under a larger magnetic field. As shown in Fig. 3(a), these faint contrasts disappear at a larger field of  $+9$  mT, indicating that all the FM moments, including those at the original FM DW, have now been aligned. However, at lower magnetic fields, the *same* faint contrasts return to the *same* locations, as can be barely observed at  $+4.2$  mT [Fig. 3(b)] and clearly observed at  $+1.2$  mT [Fig. 3(c)]. The same conclusion is reached using a negative magnetic field. When all the FM moments have been aligned at  $-9$  mT [Fig. 3(d)], the same contrasts return at  $-1.2$  mT, as shown in Fig. 3(f). To further illustrate this point, the same area in Figs. 3(c) and 3(f) has been enlarged four times, as shown on the right. The comparison shows that the structure of the FM DW has the *same* details even though the overall magnetization axes are opposite in the two cases. These results demonstrate clearly that, when a large field (e.g., 9 mT) sweeps the FM layer (including those FM moments directly above the AF DW) into alignment, the external magnetic field has no effect on the underlying AF DW. When the external field is reduced to within the lower field range of  $-2$  to  $2$  mT, the faint contrasts return and persist in the top FM layer, as shown in Fig. 2. The faint contrasts indeed mark the location of the underlying AF DW, which cannot be otherwise directly observed.

In isolated polycrystalline AF thin films, the grain size usually defines the AF domain, each of which has its own anisotropy axis. However, in FM/AF bilayers, the FM sets the anisotropy axis of the AF during field cooling. A major conclusion of our studies is that the AF domains have the *same* size as that of the FM domains. In FM/AF bilayers, using the usual field cooling under a constant magnetic field [e.g., Fig. 1(a)], there would be only one single AF domain spanning the entire sample. The stationary AF DWs in this case would be the edges of the sample, and thus cannot be

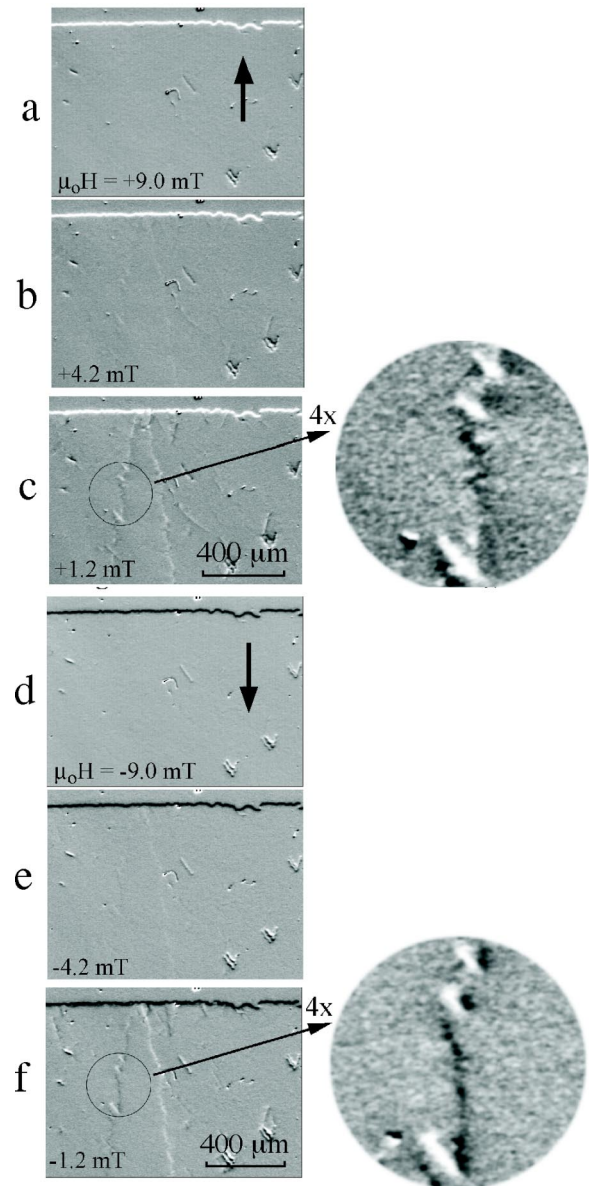


FIG. 3. MOIF images of domain patterns over the same area as in Fig. 2, but at larger magnetic field  $\mu_0 H$  of (a) 9, (b) 4.2, (c) 1.2, (d)  $-9$ , (e)  $-4.2$ , (f)  $-1.2$  mT. The black arrows indicate the magnetization direction of the domains. The same area in (c) and (f) have been enlarged four times, showing the detailed domain wall structures.

observed. It should be emphasized that the sizes of the FM domains and the AF domains here are several mm in length and a fraction of mm in width. These dimensions are three orders of magnitude larger than the grain sizes of the FM and the AF layers. The switching behavior and the domain pattern that we have observed are, therefore, unrelated to the grain sizes of the magnetic layers.

The microscopic model that encompasses the experimental results is schematically illustrated in Fig. 4. In the ground state, showing in Fig. 4(a), there are striped domains separated by the DWs. However, each DW is a *hybrid* domain wall consisting of the FM DW and the AF DW connected by a line singularity as schematically shown in Fig. 4(b), which



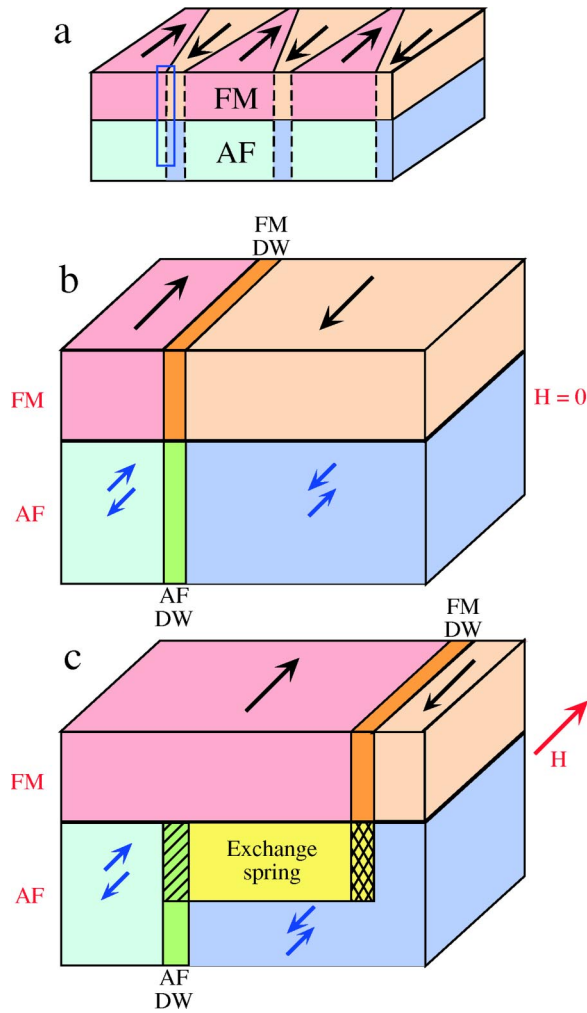


FIG. 4. (Color online) Schematic representations of the striped domain structure (a) in the ground state of the FM/AF bilayer. The boxed region in (a) is magnified in (b) showing a hybrid FM/AF domain wall consisting of the FM domain wall and the AF domain wall. (c) During reversal of the FM, an exchange spring is formed within the AF that connects to the moving FM domain wall at one end and the stationary AF domain wall at the other.

is a magnified version of the boxed region in Fig. 4(a). The external magnetic field exerts pressure on the FM DW, but not on the AF DW. As the FM DW moves, an exchange spring parallel to the interface, is formed within the AF near the interface as shown in Fig. 4(c). The exchange spring extends into the AF with a depth  $\delta$  of the order of  $(A/K)^{1/2}$ , where  $A$  and  $K$  are the exchange stiffness and anisotropy constant, respectively, of the AF, and the value of  $\delta$  for FeMn has been estimated to be of the order of tens of nm.<sup>6</sup> When the FM DW moves, it carries with it a mobile line singularity (the hatched region) in the interfacial region, while an immobile line singularity (the shaded region) remains at the location of the stationary AF. The exchange spring, bounded by these two line singularities, is connected to a moving FM DW at one side, and a stationary AF DW at the other. The mobile singularity (the hatched region) at the intersection of the FM DW, the exchange spring, and the undisturbed AF spin structure plays key roles in the bilayer magnetization processes.

It is well known that DWs move readily in isolated FM films. In exchange-coupled FM/AF bilayers, however, the moving FM DW carries with it the mobile line singularity, which reconstructs the undisturbed AF region into an exchange spring. This process impedes the FM DW motion during the winding of the exchange spring. This process continues until the FM layer is a single domain. When the external field decreases, its pressure on the FM spins lessens, such that at some critical fields, the stored energy in the exchange spring becomes sufficiently large for its unwinding. This process begins at regions where the anisotropy and exchange energies are the highest. At that, the heterogeneous FM/AF exchange spring begins to retrieve, and leading to nucleation and growth of the domains in the FM layer until the ground state is reached. It should be noted that the unwinding of the exchange spring occurs at the regions where anisotropy and energies are the highest as opposed to being the lowest during exchange spring nucleation. Thus, the unwinding of the exchange spring is not winding in reverse, but is instead occurring at different locations as observed. This is the basis for the asymmetrical reversal and the asymmetrical domain growth in exchange-coupled systems.

Finally, we discuss the origin of the domain wall orientation revealed in this work. It is known that the DW can be one of two chiralities where the spins are twisted clockwise or counterclockwise, or a mixture of both chiralities separated by the Bloch line singularities. As shown in Fig. 4(c), the moving FM DW causes an exchange spring penetrating into the AF with a depth of  $\delta$ , in which the spins are twisted according to the chirality of the FM DW. From this point on, the mobility and orientation of the FM DW is controlled by the spin singularity in the exchange spring. During reversal, the magnetic field of decreasing magnitude or of opposite sign leads to different chirality in the exchange spring, which nucleates at different locations with a different orientation.

In summary, using a FM/AF bilayer with a ground state consisting of stripe FM domains as accommodated by a special field-cooling process, we have observed features that are essential for the understanding of exchange bias. We have provided unequivocal evidences that the AF spin structure in exchange-coupled AF/FM bilayer is not static, contrary to the assumptions in some theoretical models. Our results are consistent with a microscopic model for exchange bias that involves a FM/AF exchange spring. At the ground state, all DWs are hybrid FM/AF DWs. During reversal under a magnetic field, the FM DW moves, while the AF DW remains stationary. The AF spins near the interface form an exchange spring between a moving FM domain wall and a stationary AF domain wall. The shifted hysteresis loop, the signature of exchange bias, involves winding and unwinding of the exchange spring during the backward and forward reversals.

We thank N. J. Gökemeijer for the samples. Work at JHU was supported by NSF Grants Nos. DMR00-80031 and DMR01-01814.

- <sup>1</sup>W.H. Meiklejohn and C.P. Bean, Phys. Rev. **102**, 1413 (1956); **105**, 904 (1957).
- <sup>2</sup>J. Nogues and I.K. Schuller, J. Magn. Magn. Mater. **192**, 203 (1999).
- <sup>3</sup>A.E. Berkowitz and K. Takano, J. Magn. Magn. Mater. **200**, 552 (1999).
- <sup>4</sup>R.L. Stamps, J. Phys. D **33**, R247 (2000); M. Kiwi, J. Magn. Magn. Mater. **234**, 584 (2001).
- <sup>5</sup>B. Dieny, V.S.S. Speriosu, S.S.P. Parkin, B.A. Gurney, D.R. Wilhoit, and D. Mauri, Phys. Rev. B **43**, 1297 (1991).
- <sup>6</sup>D. Mauri, H.C. Siegmann, P.S. Bagus, and E. Kay, J. Appl. Phys. **62**, 3047 (1987).
- <sup>7</sup>M.D. Stiles and R.D. McMichael, Phys. Rev. B **59**, 3722 (1999).
- <sup>8</sup>N.C. Koon, Phys. Rev. Lett. **78**, 4865 (1997).
- <sup>9</sup>T.C. Schulthess and W.H. Butler, Phys. Rev. Lett. **81**, 4516 (1998).
- <sup>10</sup>A.P. Malozemoff, Phys. Rev. B **35**, 3679 (1987); J. Appl. Phys. **63**, 3874 (1988).
- <sup>11</sup>V.I. Nikitenko, V.S. Gornakov, A.J. Shapiro, R.D. Shull, Kai Liu, S.M. Zhou, and C.L. Chien, Phys. Rev. Lett. **84**, 765 (2000).
- <sup>12</sup>H. Ohldag, A. Scholl, F. Nolting, A. Anders, F.U. Hillebrecht, and J. Stöhr, Phys. Rev. Lett. **86**, 2878 (2001).
- <sup>13</sup>N.J. Gökemeijer, J.W. Cai, and C.L. Chien, Phys. Rev. B **60**, 3033 (1999).
- <sup>14</sup>V.I. Nikitenko, V.S. Gornakov, L.M. Dedukh, Yu.P. Kabanov, A.F. Khapikov, A.J. Shapiro, R.D. Shull, A. Chaiken, and R.P. Michel, Phys. Rev. B **57**, R8111 (1998).